

Extremely short and unipolar light pulses: state of the art

N N Rosanov, M V Arkhipov, R M Arkhipov

DOI: <https://doi.org/10.3367/UFNe.2024.07.039718>

Contents

1. Introduction	1129
2. Pulse electric area and its main property	1130
3. Generation of unipolar pulses in quantum dots	1131
4. Propagation and registration of unipolar pulses	1132
5. Three-dimensional and one-dimensional schemes and models	1133
6. Conclusions	1137
References	1137

Abstract. A review of recent results in the field of short and half-cycle electromagnetic pulses is presented. The sources of their electric area, i.e., the integral of the electric field strength over time, which is the main characteristic of extremely short pulses, are brought to light. The formation of unipolar and quasi-unipolar pulses under the influence of low-cycle pulses on a quantum dot and on nested quantum wells is analyzed. A number of potential applications of unipolar electromagnetic pulses are discussed.

Keywords: unipolar electromagnetic pulses, electric area of pulses, Maxwell's equations, holography of fast processes

1. Introduction

Reducing the duration of electromagnetic pulses is necessary in order to enter the world of very fast processes and to control them. Recall that the characteristic oscillation time of atoms in simple molecules is in the femtosecond range $10^{-14} - 10^{-13}$ s = 10–100 fs (1 fs = 10^{-15} s). The motion of electrons in atoms takes place on attosecond time scales, 10^{-16} s = 100 as (1 as = 10^{-18} s). And zeptosecond times on the order of 10^{-22} s = 0.1 zs (1 zs = 10^{-21} s) characterize the processes inside the nuclei. To resolve the temporal dynamics of such processes, even shorter pulses must be applied.

Femtosecond laser pulses made it possible to observe atomic motion in molecules and the course of chemical reactions, which was the subject of the 1999 Nobel Prize in chemistry [1]. The recent Nobel Prize in physics “for experimental methods that generate attosecond pulses of

light for the study of electron dynamics in matter” [2] marks the next important step in this direction. In addition to the attosecond spectroscopy of atoms, molecules, and solids, which has been actively developed in recent years [3, 4], we mention a significant potential of such short pulses for applications. The experimentally demonstrated attosecond switching times [5, 6] allow us to talk about the electronics of petahertz frequencies (1 PHz = 10^{15} Hz), which is many orders of magnitude higher than the frequencies achieved in semiconductor electronics.

At present, the main way to obtain such short pulses is to broaden the spectrum by generating a large number of phased harmonics of the laser radiation [7, 8]. However, the ability to generate higher harmonics is limited. A further reduction in the pulse duration requires a reduction in the number of field oscillations. The limit here is set by half-cycle, unipolar pulses. Since the vector of the electric field strength in such pulses does not substantially change its direction during the main part of the pulse, unipolar pulses act unidirectionally on electric charges and are therefore more efficient than ‘usual’ bipolar pulses.

To the best of our knowledge, unipolar pulses were first mentioned in the book by Jackson [9] and then in the article by Bessonov [10] and many subsequent studies (see reviews [11–14] and the bibliography therein). The physics of such pulses is unusual and requires the development of new views based on the strict Maxwell equation and on experiments, which have not been very numerous so far. The task of this review is to describe fresh results in this field, with only minimal mention of some previous conclusions necessary for a consistent presentation. Further, in Section 2, we will introduce and discuss the main properties of the electric pulse area, a specific and the most important property for few-cycle pulses. Two sources of the nonzero electric area will also be identified here. In Section 3, we will show that a pulse with zero electric area forms a unipolar electromagnetic pulse when it hits a quantum dot with a nonlinear response. Section 4 is devoted to the propagation and detection of unipolar pulses. In Section 5, after discussing the relationship between three-dimensional and one-dimensional models of unipolar

N N Rosanov^(a), M V Arkhipov^(b), R M Arkhipov^(c)
Ioffe Institute, ul. Politekhnikeskaya 26, 194021 St. Petersburg,
Russian Federation
E-mail: ^(a) nnrosanov@mail.ru, ^(b) mikhaile.v.arkhipov@gmail.com,
^(c) arkhipovrostislav@gmail.com

Received 11 March 2024, revised 5 July 2024
Uspekhi Fizicheskikh Nauk 194 (11) 1196–1206 (2024)
Translated by S D Danilov

pulse propagation, a promising scheme for quasi-unipolar pulse generation is presented and the propagation of few-cycle pulses in a medium with a resonant response is analyzed. Dynamical gratings and resonators induced in the medium by unipolar pulses and also a nontraditional holographic scheme are discussed as examples of possible applications. The main conclusions are drawn in the last section.

2. Pulse electric area and its main property

One of the main characteristics of ultrashort electromagnetic pulses is their electric area,

$$\mathbf{S}_E(\mathbf{r}) = \int_{-\infty}^{+\infty} \mathbf{E}(\mathbf{r}, t) dt. \quad (1)$$

Here, $\mathbf{E}(\mathbf{r}, t)$ is the electric field strength at the point \mathbf{r} at time moment t . Previously, this quantity was called ‘the integral of the field over time’ [9, 10]. According to (1), the electric area is the zero frequency component of the electric field. In some cases, it is more convenient to define this quantity as the limit

$$\mathbf{S}_E(\mathbf{r}) = \lim_{\omega \rightarrow 0} \mathbf{E}_\omega(\mathbf{r}), \quad (2)$$

where

$$\mathbf{E}_\omega(\mathbf{r}) = \int_{-\infty}^{+\infty} \mathbf{E}(\mathbf{r}, t) \exp(-i\omega t) dt. \quad (3)$$

We are interested only in field distributions which are localized in time at each spatial point and localized in space at each instant of time, so fields with a nonzero static component are excluded from consideration (their electric area (1) would be infinite), as is continuous radiation (its field energy is infinite). For multi-cycle pulses, their electric area (1) is close to zero due to multiple oscillations of electric strength. Therefore, this quantity is useful only for pulses with a few oscillations. The degree of unipolarity [15]

$$\xi = \frac{|\int_{t=-\infty}^{+\infty} \mathbf{E}(\mathbf{r}, t) dt|}{\int_{t=-\infty}^{+\infty} |\mathbf{E}(\mathbf{r}, t)| dt} \quad (4)$$

is maximal for half-cycle pulses, $\xi = 1$, and it is practically zero for multi-cycle pulses.

The electric field strength is related to the vector potential \mathbf{A} as $\mathbf{E} = -\partial\mathbf{A}/\partial t$ (in the gauge with a zero scalar potential). In this case,

$$\begin{aligned} \mathbf{S}_E(\mathbf{r}) &= \int_{-\infty}^{+\infty} \mathbf{E}(\mathbf{r}, t) dt = -[\mathbf{A}(\mathbf{r}, t = +\infty) - \mathbf{A}(\mathbf{r}, t = -\infty)] \\ &= -\mathbf{A}(\mathbf{r}, t = +\infty). \end{aligned} \quad (5)$$

Here, we have assumed that, before the pulse arrives at point \mathbf{r} , the electric potential is zero, $\mathbf{A} = 0$. The electric area can therefore be interpreted as the vector potential that is preserved at the point \mathbf{r} after the pulse has ended. Note that for localized distributions of electric strength for pulses with nonzero electric areas (hereafter referred to as unipolar), the distribution of the vector potential will turn out to be nonlocalized.

If a sufficiently short pulse with electric area \mathbf{S}_E acts on a charge q , this pulse ‘pushes’ the charge, ‘instantaneously’ changing its momentum \mathbf{p} by the amount $\delta\mathbf{p} = q\mathbf{S}_E$. This can be easily seen using the classical equation for the motion of a

charge (Newton’s second law)

$$\frac{d\mathbf{p}}{dt} = q\mathbf{E}(\mathbf{r}_q, t), \quad (6)$$

where \mathbf{r}_q is the radius-vector of the point charge. The expression for $\delta\mathbf{p}$ is obtained by integrating (6) over time, provided that the charge does not shift during the pulse action at the distance where it is affected by a noticeably changed electric field. In this way, the electric area of the pulse acquires the meaning of a change in the mechanical momentum of a particle with unit charge under the action of this pulse.

This meaning of the electric area allows us to introduce its characteristic value as the one at which the pulse substantially affects the object. For this purpose, the transferred mechanical momentum δp should be compared with the characteristic mechanical momentum of the object p_0 . For a free charge, $p_0 \sim mc$, where m is the mass of the charged particle, and c is the speed of light in a vacuum. Hence, the characteristic value of the electric area $S_{E,0} \sim mc/q$ [16]. For a quantum particle of size a_0 (e.g., the radius of Bohr’s orbit), from the uncertainty relation it follows that $p_0 \sim \hbar/a_0$ (where \hbar is the reduced Planck constant). This gives $S_{E,0} \sim \hbar/qa_0$ [17].

We now turn to the main property of the electric area. For this, we use Maxwell’s electrodynamic equation, which expresses Faraday’s induction law [18]

$$\text{rot } \mathbf{E} = -\frac{1}{c} \frac{\partial \mathbf{B}}{\partial t}. \quad (7)$$

Here, \mathbf{B} is the magnetic induction. We assume that the medium was in equilibrium before the pulse action and that it returns to equilibrium once the pulse and relaxation processes have ceased. Then, integrating (7) over time, we obtain

$$\text{rot } \mathbf{S}_E = 0. \quad (8)$$

According to (8), the vector field of the electric area is irrotational and potential. In one-dimensional geometry, where the electric field strength \mathbf{E} depends only on one Cartesian coordinate z and time, (8) takes the form of the ‘conservation rule’

$$\frac{d}{dz} \mathbf{S}_E = 0 \quad (9)$$

(the applicability of one-dimensional geometry is discussed below).

Relations (8) and (9) established in [19, 20] have a number of important implications. Relation (8) allows the following paradox to be solved. As we have already pointed out, after the passage of unipolar pulses, they leave a nonuniform distribution of vector potential in the space ‘forever.’ From the Aharonov–Bohm effect [21], we know that the vector potential is an observable quantity and can be measured. A more careful investigation shows that one can measure only an integral over a closed contour which is identically equal to zero because of the potential character of the vector field of the electric area [22]. The conservation rule (9) shows that the electric area of the pulse is conserved when the pulse propagates in absorbing and amplifying, linear and non-linear, homogeneous and inhomogeneous dielectrics and conducting media. It also allows checking the correctness of approximate approaches to the description of short electromagnetic pulses, which will be briefly discussed later.

To go further in determining the distribution of electric area, we need to concretize the medium in the form of an additional material relation. In an unbounded vacuum, which has never contained electric charges or media at any point, the existence of electromagnetic field structures with nonzero electric area and finite energy is impossible [23, 24]. However, this statement is of limited value, because such a situation is only imaginary. Studies mentioned in reviews [13, 14] showed that, in a vacuum with electric charges, the source of electric area is the integral charge density $Q(\mathbf{r}) = \int_{-\infty}^{+\infty} \rho(\mathbf{r}, t) dt$, where $\rho(\mathbf{r}, t)$ is the charge density. In an electrically neutral system of charges, $\int_{-\infty}^{+\infty} \rho(\mathbf{r}, t) d\mathbf{r} = 0$, and, in the opposite case, the electric area is infinite, so to obtain the nonzero electric area of pulses it is necessary and sufficient that the integral density not be zero, at least in some subdomain of the space. In other words, a temporal separation and subsequent annihilation of opposite charges leads to the generation of a unipolar (with nonzero electric area) electromagnetic pulse.

Since no material equations characterizing the media were used to derive (8) and (9), they are rather general. Are there any limits on their applicability?

To answer this question in the affirmative, we first mention that the derivation of (8) from (7) is not affected by the presence of a steady magnetic field (the permanent magnet field). However, the form of (8) changes for a medium with a ferromagnetic hysteresis [18] when it is realized under the action of an electromagnetic pulse on the medium [25]. In fact, the magnetic induction can be written in the form $\mathbf{B} = \mathbf{H} + 4\pi\mathbf{M}$, where \mathbf{H} is the magnetic field strength and \mathbf{M} is the magnetization. If the medium has remanent magnetization \mathbf{M}_{rc} , which is preserved in the absence of external fields, the integration of (7) over time leads to a more general relation,

$$\text{rot } \mathbf{S}_E = -\frac{4\pi}{c} \delta\mathbf{M}, \quad (10)$$

where

$$\delta\mathbf{M}(\mathbf{r}) = \mathbf{M}_{rc}(\mathbf{r}, t = +\infty) - \mathbf{M}_{rc}(\mathbf{r}, t = -\infty). \quad (11)$$

In the case of remagnetization, $\delta\mathbf{M}$ is different from zero. In this case, it follows from (10) that remagnetization necessarily generates a unipolar electromagnetic pulse and that the vector field of its electric area ceases to be irrotational. This opens the possibility of generating and amplifying the electric area in media with magnetic ordering. Remagnetization can be caused by an electromagnetic (terahertz) pulse with zero electric area [26]; the switching time by a current pulse can reach 6 ps [27]. In a far field, the pulse electric area decays in inverse proportion to the square of the distance to the sample.

A qualitative example of switching in a monodomain sample under the action of an electromagnetic pulse with a zero electric area is shown in Fig. 1a [25]. Assuming for simplicity that the magnetic field in the pulse varies slowly, we can use quasi-stationary approximation to describe the dynamics of magnetic induction in the sample. Under such conditions, the electromagnetic pulse will induce switching from the initial state 1 to the finite state 6.

3. Generation of unipolar pulses in quantum dots

It follows from Section 2 that the sources of pulses with nonzero electric area are moving charges (their nonzero integral density) and remagnetization (in media with a

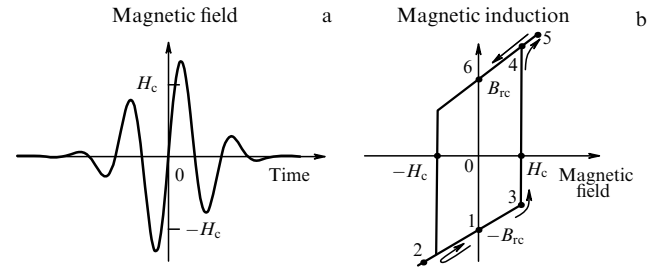


Figure 1. (a) Strength of magnetic field in an electromagnetic pulse with zero electric area incident on a monodomain sample. (b) Quasistationary magnetic hysteresis loop in a sample with coercive force H_c and change in magnetic field induction with time $1 \rightarrow 2 \rightarrow 1 \rightarrow 3 \rightarrow 4 \rightarrow 5 \rightarrow 6$.

ferromagnetic hysteresis). The above-mentioned reviews give references to experimental work and to a much larger number of theoretical studies that demonstrate the generation of such pulses by charges moving in a vacuum or crossing interfaces between media (transient radiation [28]), when pulses with zero electric areas act on a system of charges, or when such pulses are split into separate half-cycle pulses in a nonlinear medium. Here, we will present an example of the generation of a unipolar electromagnetic pulse by a bipolar pulse acting on a quantum dot [29]; we note that the discovery [30] and subsequent widespread use of quantum dots was the subject of the 2003 Nobel Prize in chemistry [31].

Suppose a bipolar electromagnetic pulse of electric strength $E_i(t)$ is incident on a semiconductor quantum dot (a nanocrystal) (see the inset in Fig. 2). The polarization of the radiation is assumed to be linear. The size of the nanocrystal is much smaller than the wavelengths considered here. This allows disregarding the coordinate dependence of the electric strength in the incident pulse and to use the dipole approximation to describe the interaction between the pulse and the quantum dot.

Exciton polarization in the quantum dot occurs when an electron jumps between the valence and conduction zones and is described by a nonlinear oscillator model for the exciton dipole moment $d(t)$ [32, 33],

$$\ddot{d} + 2\gamma\dot{d} + \omega_0^2 d + \beta d^3 = \lambda E_i(t). \quad (12)$$

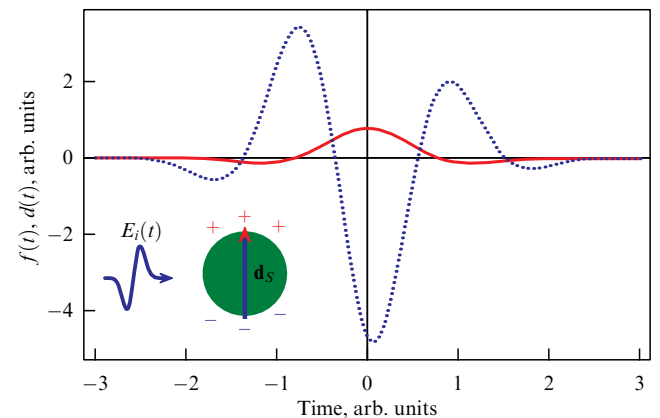


Figure 2. Time profiles of incident pulse $E_i(t)$ (dotted line) and dipole moment $d(t)$ (solid line) for parameters $\Omega = 2\omega_0$, $\alpha = \omega_0$, $\gamma = \omega_0/2$, $\hbar\beta\lambda/(2\omega_0^3) = -2$; time is measured in units ω_0^{-1} . Inset shows a quantum dot (green sphere) and profile of the incident pulse (solid blue curve).

Here, the dots denote time derivatives, the positive constant γ is the damping rate of the exciton which accounts for the recombination processes, $\hbar\omega_0$ corresponds to the width of the forbidden zone, β is the nonlinearity parameter, and λ is the coupling coefficient between the exciton and the field, which is expressed through the nanocrystal microparameters. It is assumed that the quantum dot radius exceeds the Bohr radius of the exciton, so the exciton in the nanocrystal is quantized as a whole.

The known expression for the field of a point dipole [34] after integration over time leads to the following expression for the pulse electric area:

$$\mathbf{S}_E = \frac{3(\mathbf{n}d_S)\mathbf{n} - d_S}{r^3}. \quad (13)$$

Here, $\mathbf{n} = \mathbf{r}/r$ is the unit vector in the direction from the center of the quantum dot to the observer, and $\mathbf{d}_S = \int_{-\infty}^{+\infty} d(t) dt$ is the zero-frequency component of the exciton dipole moment. This expression coincides with the asymptotic (far field) of the pulse electric area generated by a system of charges in a vacuum [13, 14].

Equation (12) directly suggests which temporal profile of the incident pulse $E_i(t)$ is needed to obtain a given profile of the dipole moment of the quantum dot $d(t)$. The additional condition $\mathbf{d}_S \neq 0$ imposes some restrictions on the parameters of the incident pulse $E_i(t)$. For example, to obtain the profile

$$d(t) = d_0 \exp(-\alpha t^2) \cos(\Omega t + \varphi) \quad (14)$$

with $\varphi \neq \pm\pi/2$, the zero-frequency component of the dipole moment is different from zero for the following relationship for the parameters:

$$\frac{\beta d_0^2}{\omega_0^2} = - \frac{4\sqrt{3} \exp[-\Omega^2/(4\alpha)] \cos \varphi}{\exp[-3\Omega^2/(4\alpha)] \cos(3\varphi) + 3 \exp[-\Omega^2/(12\alpha)] \cos \varphi}. \quad (15)$$

Figure 2 shows the time profiles of the incident pulse and the dipole moment. From this figure, it is obvious that d_S is nonzero and, correspondingly, because of (13), that the generated pulse is unipolar.

The results of the numerical solution of (12) for an incident pulse with the profile

$$E_i(t) = E_0 \exp\left(-\frac{t^2}{\tau^2}\right) \sin(\Omega t) \quad (16)$$

are shown in Fig. 3. Naturally, the unipolarity of the generated pulse appears only in the presence of nonlinearity (exciton–exciton interaction) $\beta \neq 0$. The absolute value $|d_S|$ increases together with the absolute value of nonlinearity $|\beta|$. The nonmonotonic dependence of $|d_S|$ on the distance from the resonance frequency is also worth mentioning.

4. Propagation and registration of unipolar pulses

The spectrum of unipolar half-cycle pulse lies in the range from the maximum bounding frequency to the zero frequency. Every optical system contains elements of a finite size, such as an aperture, a lens, or a mirror. These elements are obstacles in the path of low-frequency components present in unipolar radiation. For example, a concave mirror or lens will not focus the spectral components with a

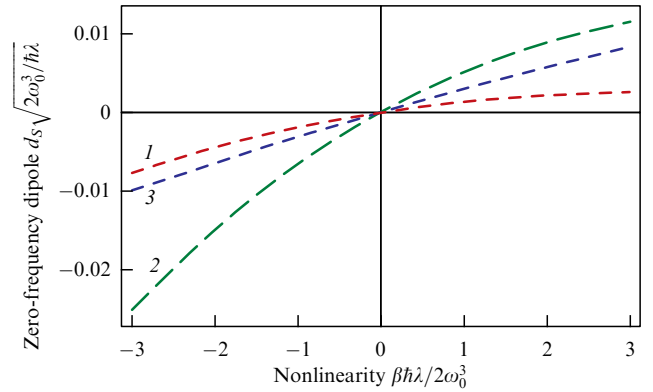


Figure 3. Dependence of zero-frequency component of dipole moment of quantum dot d_S induced by the field pulse (16) on nonlinearity coefficient β for different values of ‘carrier frequency’ of incident pulse Ω . Dimensionless frequency $\Omega/\omega_0 = 1$ (curve 1), 2 (2), and 3 (3). Other parameters are fixed: $\omega_0\tau = 1$, $2\lambda E_0^2/(\hbar\omega_0^4) = 1$.

wavelength that is comparable to or exceeds their size. Therefore, even if the radiation is unipolar near the source of finite size, it ceases to be unipolar in the far field due to the reduction in the low-frequency part and the suppression of the zero-frequency component. As a result, an initially unipolar half-cycle pulse loses its unipolarity in an optical system or in a free space.

How can this difficulty be overcome? The recipe is well known in radio communications and in the localization of ‘nonsinusoidal waves’ [35] and consists in the following. Half-cycle and unipolar pulses in the far zone can be obtained if the current in antennas has a stepwise dependence on time instead of the usual harmonic one. Then, the time derivative of the current defining the far zone will have the form of a short peak with a duration equal to that of the jump in the step.

For a single field peak in the far field zone, the current in the antenna should continue infinitely long after the step, which is practically unrealizable. If the current in the antenna is interrupted, the current pulse acquires a trapezoidal form. Then, two pulses of opposite polarity are observed in the far field. The interval between them is equal to the duration of the apex of the trapezoid. The radiation will not be unipolar, but each pulse taken separately will be. It can be very short, with a wide spectrum. This is the reason why radars with nonsinusoidal signals are currently called ‘ultrabroadband,’ and they have many advantages [36]. Such a source has not yet been realized in the optical and adjacent bands. However, this example shows that it is possible in principle.

Experimental studies on the generation and application of unipolar pulses will inevitably require methods and instruments to identify unipolarity and measure the electric area. At present, there is no commercial instrument available for solving these tasks. Therefore, it is worthwhile to briefly discuss the principles of constructing such instruments.

An obvious and direct way to solve this task is to measure the time dependence of the electric field and then calculate the integral (1). However, there is no direct way to measure this dependence in the optical or adjacent bands. In the terahertz band, such a method is realized for a number of sources. For nonlinear-optical pulse generation methods, the dependence we are interested in can be obtained using electrooptical detection schemes. If the unipolarity is lost in the detection system due to the finite size of the optical elements or the

small distance to the source, this can be taken into account in the mathematical processing. A demonstration of the unipolarity of radiation near the source by processing was carried out in [37]. The processing procedure consists of integrating the experimental dependence of the electric field in the far field region with a variable upper limit, which allows its temporal form to be computed, which is proportional to the field in the near field region. In Ref. [38], an original method of field detection in the near field was realized that avoids this integration procedure, and the existence of a unipolar pulse-forerunner was demonstrated by generating terahertz pulses in nonlinear crystals. It is also shown there that the pulses of the forerunner have an almost rectangular temporal dependence of the electric field. The authors demonstrated that the pulse profile changes and the unipolarity is lost as the pulse propagates in free space, due to the reduction of a low-frequency fraction and the disappearance of the zero-frequency component in its spectrum.

The second approach is based on radio techniques. To detect low frequencies and unipolarity, a small radio antenna connected to the DC input of an oscilloscope can be used. This approach has been used to demonstrate unipolarity in the terahertz range in [37].

A demonstrable example of the existence of unipolar radiation in a natural phenomenon can be mentioned: lightning during a thunderstorm. Here, the radiation spectrum includes frequencies from radio to X-ray. And the whole set of electric fields, from the radiation of individual atoms to the field created by the collective directed motion of charges, can have a nonzero electric area. To demonstrate this fact, let us take an oscilloscope. To observe the temporal shape of the field strength, we connect a cable to the oscilloscope operating in the waiting mode, using the cable free end as an antenna. A warning: such experiments are not without danger.

When a thunderstorm is approaching, the oscilloscope sweep appears almost immediately with the thunder, and the character of the pulses varies. Some of the pulses have a well-defined unipolar form. To establish the unipolarity, it is necessary to integrate the oscilloscope signal, as mentioned above. An example of an oscillogram and its processing is shown in Fig. 4.

The cause of unipolarity is well known. Lighting discharges usually consist of a unidirectional current pulse passing through a long (from several hundred meters to kilometers) narrow plasma channel in Earth's atmosphere. The directional current pulse generates an electromagnetic pulse. The pulse is unipolar in the vicinity of discharge. It becomes bipolar far from it. In laboratory conditions, one can see in a similar way that analogs of

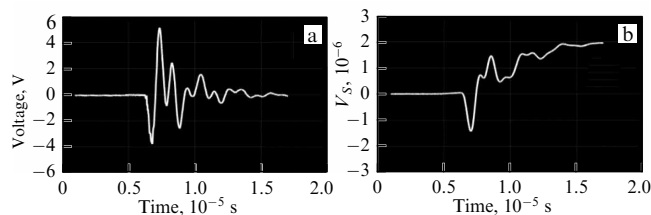


Figure 4. (a) Oscilloscope of voltage at exit of coaxial cable during a thunderstorm. (b) Numerical integration of oscilloscope (a) with a variable upper limit, which shows the presence of unipolarity in original signal (a).

lighting—pulse flashes fed by DC voltage—create unipolar pulses in the near field.

5. Three-dimensional and one-dimensional schemes and models

Coaxial waveguides. In Section 4, it was pointed out that, in free space, initially unipolar pulses become bipolar due to diffraction acting as they propagate. It is impossible to avoid such manifestation of diffraction by using simple waveguides with a cutoff frequency—waves with frequencies below the critical one will not propagate in them. However, there is no cutoff frequency in the coaxial waveguides which are widely used in radio engineering. In such waveguides, fundamental waves of any frequency propagate at the speed of light (in a hollow waveguide) between two coaxial metal surfaces. Unipolar pulses can propagate over large distance in such waveguides [39].

This property of coaxial cables is confirmed by a rather simple experiment. A unipolar pulse generated by a fast photodiode that detects short pulses of radiation from a titanium–sapphire laser is transmitted through a long coaxial cable with virtually no change in shape. An example of the oscillogram is shown in Fig. 5. The pulse duration at the half-amplitude level for the directly connected diode (Fig. 5a) does not exceed 100 ps, according to our estimates. This corresponds to a spatial pulse width of 3 cm. The cable length of 3 m exceeds this value by a factor of 100. The shape of the detected pulses changes only slightly after passing through such a long cable, as shown in Fig. 5b. The amplitude decreases, and the duration increases slightly. However, the unipolarity of the pulse transmitted through the cable is preserved. The pulses are compared in Fig. 5c.

Quasi-unipolar pulses. Remarkably, when the transverse structure of the fundamental waves is fixed, their amplitude satisfies a one-dimensional wave equation. This supports the one-dimensional consideration of the propagation of extremely short pulses that is popular in the literature. However, the conservation rule (9), valid in the absence of ferromagnetic hysteresis, limits the use of further simplifications in the theory. In particular, the widely used ‘approx-

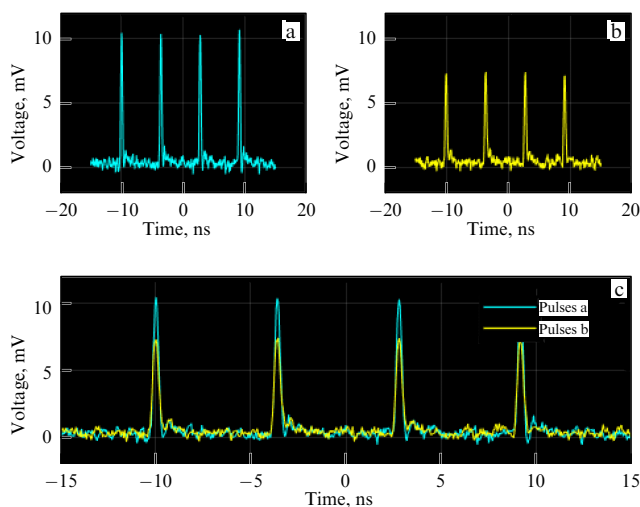


Figure 5. Oscilloscope of pulses from a photodiode registering short laser pulses, connected directly to an oscilloscope (a) and via a 3-meter coaxial cable (b); a comparison of these pulses (c).

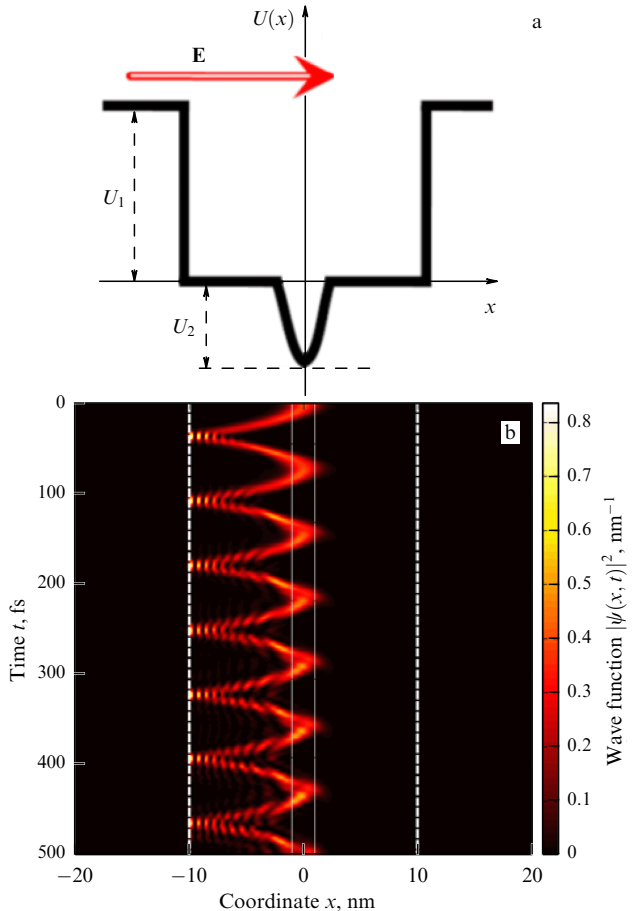


Figure 6. (a) Nested quantum well and (b) motion of wave packet inside it.

imation of unidirectional propagation' [40] can lead to qualitatively incorrect conclusions [41], as shown in [42, 43]. Indeed, as follows from (7), for linearly polarized radiation, the derivative $\partial E/\partial z$ should be proportional to $\partial B/\partial t$. Therefore, $\partial E/\partial z$ should be proportional to the time derivative of the function of the electric field strengths and their derivatives, which is not observed in [41]. In the theoretical results presented below, the approximation of one-dimensional propagation is used so that the conservation rule is maintained.

It is difficult to obtain strictly unipolar pulses in practice, and quasi-unipolar pulses become practically significant. For example, radiation may have two half-cycle pulses of different polarity separated by a time interval which is much longer than the pulse duration. In such cases, the effect of such radiation on matter can be considered to be the effect of isolated unipolar pulses if the medium, figuratively speaking, manages 'to forget' the effect of the first half-cycle until the action of the second one. Another situation occurs when a pulse has a short unipolar peak of high amplitude accompanied by long fronts of other polarity of low amplitude. If the action is nonlinear in electric strength, the long low-amplitude fronts do not manifest themselves.

A specific motion of charges in the source is required to excite half-cycle pulses, produced when rapid current changes occur on short time scales, when uniformly and straightly moving charges are decelerated or accelerated. In the picture of field lines, a characteristic bend is formed — a unipolar half-cycle pulse of radiation.

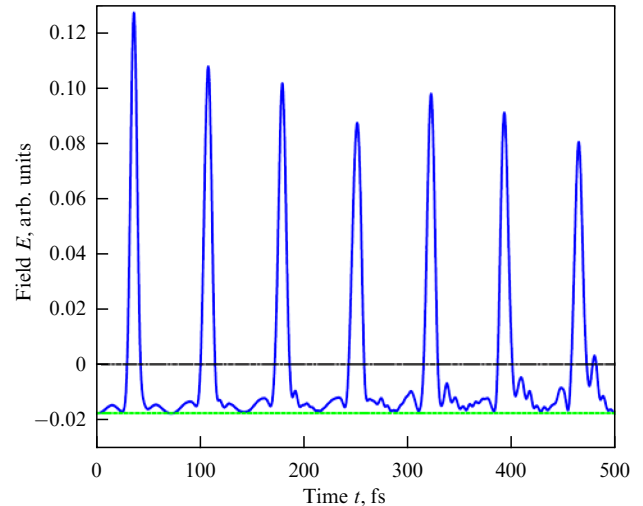


Figure 7. Dependence of electric field strength in far field on time (quasi-unipolar radiation pulses).

In terahertz photonics, short laser pulses excite unidirectional currents in semiconductors [44]. Powerful short laser pulses eject electrons from metals. The electrons are accelerated as they interact with the radiation and become sources of half-cycle pulses [45]. At present, such experimental setups are large and complex. Of interest are simple quantum systems that can directly generate half-cycle pulses, such as atoms or molecules. One such variant is the sequence of half-cycle femtosecond pulses in a structure of quantum cells in the form of nested quantum wells [46].

The idea of the method is to force an electron in a quantum system to perform an anharmonic periodic oscillatory motion in a confining potential. To realize such a potential, a structure consisting of two nested quantum wells has been proposed (Fig. 6). In this structure, a shallow quantum well is nested within a much deeper quantum well. The presence of the second quantum well allows, on the one hand, the ground state wave function to be confined within it and, on the other hand, compensating for the spectral broadening of the moving electron wave packet.

Initially, a charge is located in the shallow well with the depth U_2 ; under the action of a field pulse E , the charge enters into the outer well with the depth U_1 and steep walls and performs a bounded periodic motion. The charge cannot leave it. Figure 6 shows the motion of the wave packet of the charged particle with the mass and charge of the electron. Each time it is reflected from the boundary of the outer quantum well, a half-cycle pulse is excited that is proportional to the acceleration of the electron wave packet. The dependence of the field strength on time is shown in Fig. 7. The shape of the potential used in the calculations allows the formation of half-cycle pulses shorter than 10 fs (about 7 fs in the given example) with an ultrahigh repetition frequency of 10 THz under the following parameters: $U_1 = 2$ eV, $L_1 = 20$ nm, $U_2 = 0.06$ eV, $L_2 = 2$ nm, and $E = 10^8$ V m $^{-1}$. Here, L_1 and L_2 are the sizes of the outer and inner wells, respectively.

Profiled unipolar pulses. The ability to change the shape of half-cycle pulses extends their use for ultrafast control of the dynamics of quantum systems [47–50]. One of the approaches is the method of Fourier synthesis of pulse profiles [51]. It is based on the manipulation of phases and

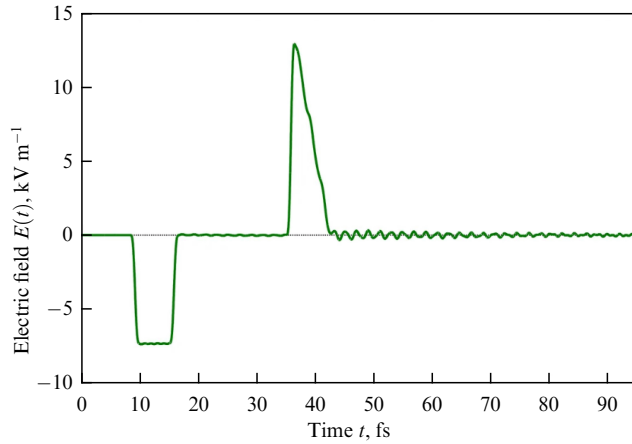


Figure 8. Field strength of radiation formed by a layer of medium. Spatial density of matter in bounding layer with a thickness of $2\ \mu\text{m}$ increases linearly, is constant inside layer with a thickness of $2\ \mu\text{m}$, and decreases to zero quadratically in next bounding layer also with a thickness of $2\ \mu\text{m}$. Linear increase gives an approximately rectangular pulse, and quadratic decrease gives a triangular pulse.

amplitudes of spectral components within a very broad spectrum.

One can manipulate the shape of half-cycle pulses by passing them through nonlinear media [52, 53]. Assume that the delay between two short half-cycle pulses is equal to the half period of the resonance transition in the particles of the medium. Oscillations of the medium polarization at the transition frequency are excited by the first pulse and are quenched by the second. In this way, a half-wave of polarization is formed.

When propagating in a spatially homogeneous medium, such a half-wave of polarization does not excite radiation. However, in the case of spatially inhomogeneous matter distribution, the amplitude of this wave varies as it propagates, resulting in the emission of unipolar pulses with different temporal profiles depending on the profile of the inhomogeneity (Fig. 8).

Half-cycle pulses in a resonant absorbing medium. Previous studies on the propagation of few-cycle pulses, carried out for the model of a two-level absorbing medium [54, 55], showed a certain analogy to the situation when multi-cycle pulses propagate coherently in the self-induced transparency (SIT) regime, when the area theorem of McCall and Hahn is valid [56–59]. However, in the case of ultrashort and even unipolar pulses, the notion of envelope loses its meaning. For this reason, to describe pulse propagation, the full system of Maxwell–Bloch equations for a multi-level medium must be solved, taking into account relaxation, which gives a more realistic picture of the interaction of such radiation with matter.

Numerical simulations of the propagation of a half-cycle unipolar pulse in a three-level absorbing medium, performed in [60], are the next step after the two-level model and reveal some differences compared to the two-level medium. For example, a half-cycle pulse that acts as a 4π pulse SIT for the main transition 1–2 in the two-level medium and decays into two pulses there propagates as a 6π pulse and decays into three pulses in a three-level medium.

An example of the space-time dynamics of the electric field in a three-level medium is shown in Fig. 9. In this example, a unipolar pulse with a shape given by a hyperbolic

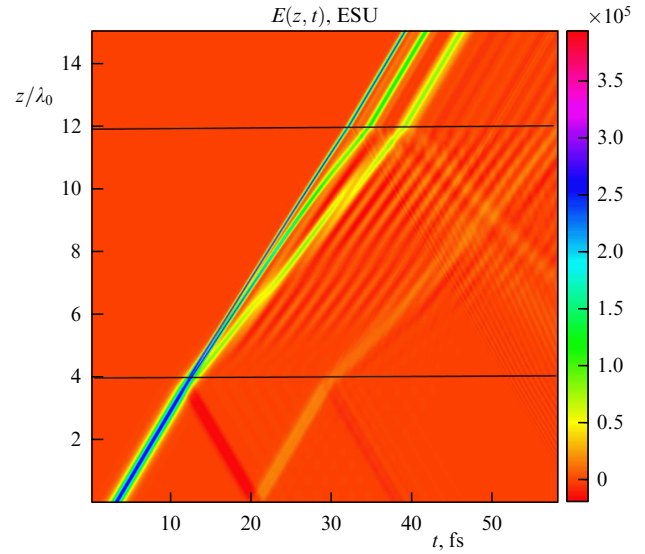


Figure 9. Spatiotemporal dynamics of electric field $E(z, t)$ in a three-level medium. Medium is located between boundaries denoted by two lines $z_1 = 4\lambda_0$ and $z_2 = 12\lambda_0$. $\lambda_0 = 700\ \text{nm}$ is wavelength of resonant transition 1–2 in the three-level medium.

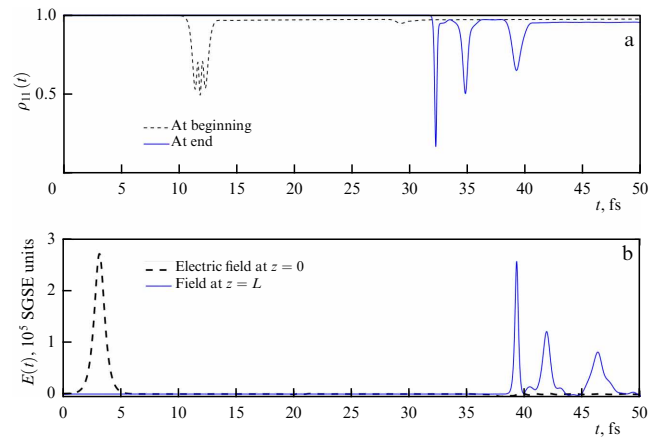


Figure 10. (a) Time dependence of medium ground state population; dashed line corresponds to beginning of the medium and solid blue line corresponds to its end. (b) Time dependence of electric field $E(t)$ in left part of integration domain $z = 0$ (dashed line) and right part $z = L$ (solid line on the right).

secant, $E(t) = E_0 \operatorname{sech}((t - z/c)/\tau)$, enters the medium. Its amplitude $E_0 = 2.7 \times 10^5$ ESU and duration $\tau = 380$ as, chosen so that it acts as a 4π pulse for the transition 1–2 in the two-level medium. The time dependence of the ground state population at the entrance to and exit from the medium, as well as the time dependence of the electric field on time at the beginning and end of the integration domain, are shown in Fig. 10.

Numerical simulations have shown that the initial pulse in the medium is split into three pulses with durations that are substantially smaller than that of the initial pulse. They propagate in the medium with different speeds (see Figs 9 and 10). Each of these pulses acts so that the medium is first excited and then returns to the initial state (see Fig. 10). This example illustrates possible transformations, in particular, the compression and multiplication of half-cycle pulses that accompany nonlinear propagation in multilevel media. Note

that the simulations confirm the conservation of electric area in accordance with (9).

Dynamical gratings and microresonators. Ultrashort pulses offer the possibility of generating and ultrafast controlling of the population difference gratings and microresonators when these pulses interact coherently with the medium, provided that the duration of these pulses is shorter than the medium relaxation time. Typically, atomic population gratings are created by the interference of crossing monochromatic beams in a resonant medium [61]. Such gratings may find numerous practical applications in optics and spectroscopy. We note that similar gratings have previously been studied in the case of multi-cycle pulses [62] that do not intersect in the medium and have been applied in echo holography [63].

However, these methods of grating generation do not allow their parameters to be modified quickly enough. To achieve this goal, ultrashort light pulses can be conveniently used. As shown earlier, the coherent propagation of ultrashort light pulses in a resonant medium can excite and modify ultrafast the grating parameters on the time scale of the pulse duration [64, 65].

An example of the dynamics of such gratings is shown in Fig. 11, where a sequence of half-cycle attosecond pulses acts on a two-level medium. The numbers of pulses entering the medium at particular times are labeled with numbers. The arrows indicate the direction of propagation for a pulse with a given number. This example confirms the possibility of generating, deleting, and multiplying the spatial period of gratings at subfemtosecond time intervals. Similar grating dynamics are also possible in a multilevel medium [65].

Available studies have also shown the possibility of excitation and control of dynamical microresonators in a resonant medium. These structures arise when ultrashort pulses collide in a medium. In this case, the population has a constant value in the region of pulse intersection [66], and on both its sides a Bragg type population grating is formed. In this sense, we can say that a resonator with Bragg mirrors is formed in the medium. Such structures can be used as fast optical switches and in light storage systems. Note also that

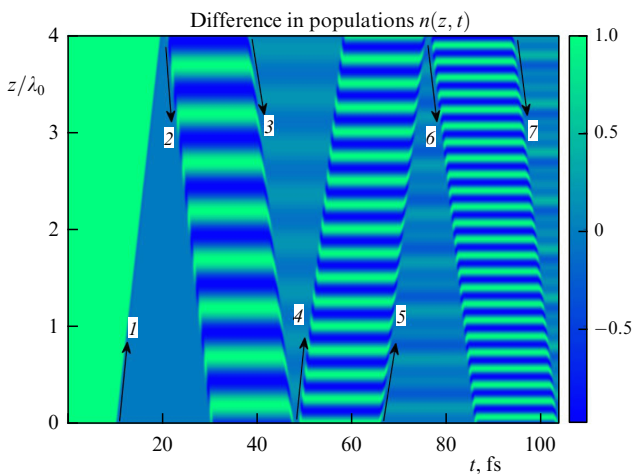


Figure 11. Spatiotemporal dynamics of difference in populations showing possibility of generation, removal, and multiplication of spatial frequency of gratings under the action of a sequence of half-cycle pulses of Gaussian shape in a two-level medium, $E(t) = E_0 \exp(-t^2/\tau^2)$. Amplitude of pulses $E_0 = 3 \times 10^7 \text{ V cm}^{-1}$, their duration $\tau = 380 \text{ as}$. Wavelength of resonant transition $\lambda_0 = 700 \text{ nm}$.

such a quasi-resonator can be created for coherent propagation of a single pulse in an optically dense medium. This leads to the appearance of an interesting phenomenon—self-stopping of light [67].

Media in which such gratings are formed can serve as examples of so-called spatiotemporal photonic crystals (STPCs), i.e., media in which the refractive index varies in space and time, or photonic time crystals (PTCs), i.e., media in which the refractive index varies rapidly with time. In recent years, such media have been the subject of active research in optics [68, 69]. One of their possible applications is the creation of threshold-less laser sources [70].

The realization of a rapidly varying refractive index in a medium is a complex task, because nonlinear optical processes are usually rather slow. Various exotic materials are used for this purpose [71, 72]. In the above examples, the gratings are created by coherent interaction of ultrashort pulses with a medium, which occurs when the duration of the light pulses and the time intervals between them are shorter than the relaxation time of the medium polarization T_2 [64, 65, 73–75]. This mechanism can be used to form gratings, i.e., the realization of STPC in atomic media under the action of ultrashort pulses [75].

Holography. Practical applications, so far only potential, of short unipolar pulses are based on the peculiarities of their action on microobjects and matter. This opens up many new possibilities and breaks the common stereotypes. One such example is holography. Let us consider what the use of unipolar pulses can bring to holography and how its framework will change.

It is usually assumed that holography necessarily requires mutual coherence between the object and reference beams in the hologram recording domain to form the interference pattern. The interference pattern remains in the recording medium, stored in its optical properties, which change proportionally to the light intensity. This imposes limitations on the object displacements when the hologram is recorded. They should be small. The duration of the radiation pulses should be long enough for the reference and object beams to cross in the recording medium. As a result, short pulses consisting of a few cycles, and even more so half-cycle pulses, seem to be inapplicable in holography.

Figure 12 shows a schematic for recording a hologram in incident beams for three types of radiation—monochromatic, pulsed multi-cycle, and unipolar half-cycle. In a medium such as a holographic photographic plate, the interference pattern between the object wave reflected from the object and the reference wave passing through the plate

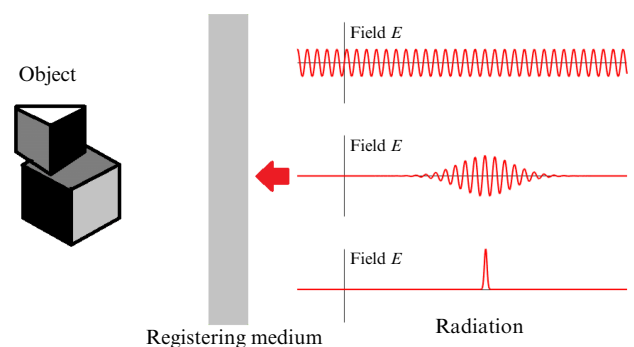


Figure 12. Schematic of a hologram registration in oppositely directed beams.

should be recorded. Obviously, in the first two cases, the limitations mentioned above apply, while a unipolar pulse cannot be used for holographic registration in the photographic plate. Let us replace the photographic plate by a resonant medium with a large time of phase memory T_2 and use only a unipolar pulse. It will excite coherent movements of dipoles in particles of the recording medium in the whole illuminated domain. A polarization wave will be excited there. It is formed by concerted oscillations of the dipole moments of the particles in the medium, which are phase-shifted depending on their spatial positions. The polarization wave will propagate behind the pulse. The radiation scattered by the object will move to meet this wave. Depending on the phase of the oscillating dipole moments of the particles, the pulse of radiation scattered by the object either amplifies or dampens the oscillations of the dipoles, i.e., excites or reduces the excitation of the medium. Thus, a grating of level population difference is created. The spatial distribution of the difference in population is fully consistent with the pattern of interference that would have occurred in an analogous stationary holographic scheme using a suitable coherent monochromatic source [76].

Note that, in traditional holography, coherence of the radiation is required, but coherence in the medium is not important. The situation is reversed in the case considered here. The medium needs coherence (a larger time T_2 of polarization relaxation due to resonant transitions), in the absence of coherence in the radiation understood in the usual way. Thus, using unipolar subcycle pulses and resonant media with a large relaxation time T_2 , it is possible to realize holography with ultrahigh temporal resolution in the absence of coherence between the reference and object beams. This allows one to perform holographic registration of rapidly changing or moving objects with ultrahigh temporal resolution.

6. Conclusions

Maxwell's electrodynamic equations show that the source of unipolarity of electromagnetic pulses is the integral density of electric charges and remagnetization. In the first case, the unipolarity is guaranteed by the temporal separation and subsequent annihilation of opposite charges. In the second case, the remagnetization can be expressed as a reorientation of molecular currents as well as spins in particles of the medium. Mastering the optics of unipolar pulses requires that we abandon some common views and develop new ideas and new theoretical and experimental methods. We clarify that we refer to pulses as field structures that exist in a spatial domain of interest only for a limited time interval.

An important characteristic of pulses of duration smaller than the time scale of microobjects interacting with the field is the electric area—the integral of the electric field strength over time. Namely, the electric area determines the efficiency of such interaction. The vector field of the electric area in media without ferromagnetic hysteresis is irrotational and subject to the 'conservation rule,' which allows checking the correctness of approximate methods used to describe the propagation of few-cycle pulses. In the vicinity of the respective sources, the unipolarity can be manifested in nanooptics. The unipolar pulses propagate as fundamental waves in coaxial waveguides and are efficiently described by a one-dimensional wave equation.

In nonlinear optical media, few-cycle pulses can be split into separate half-cycle unipolar pulses, allowing us to speak of half-cycle pulses as elementary components of bipolar pulses. The transformation of initial bipolar pulses into unipolar pulses or into quasi-unipolar pulses, with separated and nearly independent unipolar pulses, achieved in such media is sufficient to improve the efficiency of the pulse action on microobjects.

At the present time, the proposed and demonstrated methods of generating unipolar and quasi-unipolar pulses deal with a predominantly low-frequency (terahertz) spectral band. The problem of efficient generation of similar optical pulses remains open. The importance of solving this problem is emphasized by a number of unique applications of such pulses, including the holography of very fast processes.

The authors thank M M Glazov and A V Pakhomov for the useful discussions.

The analysis in Section 2 was supported by the State Assignment to the Ioffe Institute, theme 0040-2019-0017. The remaining studies were supported by the Russian Science Foundation, grant 23-12-00012.

References

1. The Nobel Prize in Chemistry 1999 ±. Summary, <https://www.nobelprize.org/prizes/chemistry/1999/summary/>
2. The Nobel Prize in Physics 2023. Press release, <https://www.nobelprize.org/prizes/physics/2023/press-release>
3. Borrego-Varillas R, Lucchini M, Nisoli M *Rep. Prog. Phys.* **85** 066401 (2022)
4. He Lixin et al. *Chin. Phys.* **31** 123301 (2022)
5. Hassan M Th *ACS Photonics* **11** 334 (2024)
6. Hui D et al. *Sci. Adv.* **9** eadf1015 (2023)
7. Sansone G, Poletto L, Nisoli M *Nature Photon.* **5** 655 (2011)
8. Ryabikin M Yu, Emelin M Yu, Strelkov V V *Phys. Usp.* **66** 360 (2023); *Usp. Fiz. Nauk* **193** 382 (2023)
9. Jackson J D *Classical Electrodynamics* (New York: J. Willey, 1962); Translated into Russian: *Klassicheskaya Elektrodinamika* (Moscow: Mir, 1965)
10. Bessonov E G *Sov. Phys. JETP* **53** 433 (1981); *Zh. Eksp. Teor. Fiz.* **80** 852 (1981)
11. Rosanov N N, Arkhipov R M, Arkhipov M V *Phys. Usp.* **61** 1227 (2018); *Usp. Fiz. Nauk* **188** 1347 (2018)
12. Arkhipov R M, Arkhipov M V, Rosanov N N *Quantum Electron.* **50** 801 (2020); *Kvantovaya Elektron.* **50** 801 (2020)
13. Rosanov N N *Phys. Usp.* **66** 1059 (2023); *Usp. Fiz. Nauk* **193** 1127 (2023)
14. Rosanov N N, Arkhipov M V, Arkhipov R M, Pakhomov A V, in *Teragertsovaya Fotonika* (Terahertz Photonics) (Eds V Ya Panchenko, A P Shkurinov) (Moscow: Russian Academy of Sciences, 2023) p. 360, collective monograph
15. Arkhipov R M et al. *JETP Lett.* **105** 408 (2017); *Pis'ma Zh. Eksp. Teor. Fiz.* **105** 388 (2017)
16. Rosanov N et al. *Phys. Rev. A* **104** 063101 (2021)
17. Arkhipov R M et al. *JETP Lett.* **114** 129 (2021); *Pis'ma Zh. Eksp. Teor. Fiz.* **114** 156 (2021)
18. Landau L D, Lifshitz E M *Electrodynamics of Continuous Media* (Oxford: Pergamon Press, 1984); Translated from Russian: *Elektrodinamika Sploshnykh Sred* (Moscow: Nauka, 1982)
19. Rosanov N N *Opt. Spectrosc.* **107** 721 (2009); *Opt. Spektrosk.* **107** 761 (2009)
20. Rosanov N N *Dissipativnye Opticheskie Solitony. Ot mikro- k nano- i atto-* (Dissipative Optical Solitons. From Micro- to Nano- and Atto-) (Moscow: Fizmatlit, 2011)
21. Aharonov Y, Bohm D *Phys. Rev.* **115** 485 (1959)
22. Arkhipov R M, Arkhipov M V, Rosanov N N *JETP Lett.* **111** 668 (2020); *Pis'ma Zh. Eksp. Teor. Fiz.* **111** 794 (2020)
23. Plachenov A B, Rosanov N N *Radiophys. Quantum Electron.* **65** 911 (2023); *Izv. Vyssh. Uchebn. Zaved. Radiofiz.* **65** 1003 (2022)

24. Feshchenko R M *J. Exp. Theor. Phys.* **136** 406 (2023); *Zh. Eksp. Teor. Fiz.* **163** 461 (2023)
25. Rosanov N N *Opt. Lett.* **49** 1493 (2024)
26. Song D et al. *Ultrafast Sci.* **3** 0007329 (2023)
27. Jhuria K et al. *Nat. Electron.* **3** 680 (2020)
28. Ginzburg V L, Frank I M *J. Phys. USSR* **9** 353 (1945); Russian extended version: *Zh. Eksp. Teor. Fiz.* **16** 15 (1946)
29. Glazov M M, Rosanov N N *Phys. Rev. A* **109** 053523 (2024)
30. Ekimov A I, Onushchenko A A *JETP Lett.* **34** 345 (1981); *Pis'ma Zh. Eksp. Teor. Fiz.* **34** 363 (1981)
31. The Nobel Prize in Chemistry 2023. Aleksey Yekimov. Facts, <https://www.nobelprize.org/prizes/chemistry/2023/yekimov/facts/>
32. Ivchenko E L *Optical Spectroscopy of Semiconductor Nanostructures* (Harrow, UK: Alpha Science, 2005)
33. Poddubny A N, Glazov M M, Averkiev N S *New J. Phys.* **15** 025016 (2013)
34. Born M, Wolf E *Principles of Optics* (Cambridge: Cambridge Univ. Press, 2019); Translated into Russian: *Osnovy Optiki* (Moscow: Nauka, 1970)
35. Harmuth H F *Nonsinusoidal Waves for Radar and Radio Communication* (New York: Academic Press, 1981); Translated into Russian: *Nesinusoidal'nye Volny v Radiolokatsii i Radiosvyazi* (Moscow: Radio i Svyaz', 1985)
36. Taylor J D *Introduction to Ultra-Wideband Radar Systems* (Boca Raton, FL: CRC Press, 2020) <https://doi.org/10.1201/9781003068112>
37. Arkhipov M V et al. *JETP Lett.* **115** 1 (2022); *Pis'ma Zh. Eksp. Teor. Fiz.* **115** 3 (2022)
38. Ilyakov I E et al. *Opt. Express* **30** 14978 (2022)
39. Rosanov N N *Opt. Spectrosc.* **127** 1050 (2019); *Opt. Spektrosk.* **127** 960 (2019)
40. Kolesik M, Moloney J V *Phys. Rev. E* **70** 036604 (2004)
41. Bogatskaya A V, Popov A M *JETP Lett.* **118** 296 (2023); *Pis'ma Zh. Eksp. Teor. Fiz.* **118** 291 (2023)
42. Pakhomov A V et al. *JETP Lett.* **119** 94 (2024); *Pis'ma Zh. Eksp. Teor. Fiz.* **119** 100 (2024)
43. Rosanov N N et al. *Opt. Spectrosc.* **132** 128 (2024); *Opt. Spektrosk.* **132** 142 (2024)
44. Lepeshov S A et al. *Laser Photon. Rev.* **11** 1600199 (2017)
45. Fülöp J A, Tzortzakis S, Kampfrath T *Adv. Opt. Mater.* **8** 1900681 (2020)
46. Arkhipov M V et al. *Opt. Lett.* **48** 4637 (2023)
47. Cirmi G et al. *Laser Photon. Rev.* **17** 2200588 (2023)
48. Hassan M Th et al. *Nature* **530** 66 (2016)
49. Bastrakova M V, Klenov N V, Satanin A M *Phys. Solid State* **61** 1515 (2019); *Fiz. Tverd. Tela* **61** 1565 (2019)
50. Arkhipov R et al. *Opt. Express* **28** 17020 (2020)
51. Hassan M Th et al. *Rev. Sci. Instrum.* **83** 111301 (2012)
52. Pakhomov A et al. *Phys. Rev. A* **106** 053506 (2022)
53. Pakhomov A et al. *Opt. Lett.* **48** 6504 (2023)
54. Arkhipov R M, Rosanov N N *Opt. Spectrosc.* **124** 726 (2018); *Opt. Spektrosk.* **124** 691 (2018)
55. Arkhipov R et al. *J. Opt. Soc. Am. B* **38** 2004 (2021)
56. McCall S L, Hahn E L *Phys. Rev.* **183** 457 (1969)
57. Kryukov P G, Letokhov V S *Sov. Phys. Usp.* **12** 641 (1970); *Usp. Fiz. Nauk* **99** 169 (1969)
58. Allen L, Eberly J H *Optical Resonance and Two-Level Atoms* (New York: Wiley, 1975); Translated into Russian: *Opticheskie Rezonansy i Dvukhurovnevye Atomy* (Moscow: Mir, 1978)
59. Poluektov I A, Popov Yu M, Roitberg V S *Sov. Phys. Usp.* **17** 673 (1975); *Usp. Fiz. Nauk* **114** 97 (1974)
60. Arkhipov R M, Pakhomov A V, Arkhipov M V, Rosanov N N *J. Exp. Theor. Phys.* **139** (2) (2024) in press; *Zh. Eksp. Teor. Fiz.* **166** 174 (2024)
61. Eichler H J, Günter P, Pohl D W *Laser-Induced Dynamic Gratings* (Springer Series in Optical Sciences, Vol. 50) (Berlin: Springer-Verlag, 1986)
62. Moiseev S A, Shtyrkov E I *Sov. J. Quantum Electron.* **21** 403 (1991); *Kvantovaya Elektron.* **18** 447 (1991)
63. Shtyrkov E I *Opt. Spectrosc.* **114** 96 (2013); *Opt. Spektrosk.* **114** 105 (2013)
64. Arkhipov R M et al. *Opt. Lett.* **41** 4983 (2016)
65. Arkhipov R et al. *Sci. Rep.* **11** 1961 (2021)
66. Diachkova O O et al. *Opt. Commun.* **538** 129475 (2023)
67. Arkhipov M, Arkhipov R, Babushkin I, Rosanov N *Phys. Rev. Lett.* **128** 203901 (2022)
68. Sharabi Y et al. *Optica* **9** 585 (2022)
69. Boltasseva A, Shalaei V M, Segev M *Opt. Mater. Express* **14** 592 (2024)
70. Xu K et al. *Opt. Lett.* **49** 842 (2024)
71. Lustig E et al. *Nanophotonics* **12** 2221 (2023)
72. Saha S et al. *Opt. Express* **31** 8267 (2023)
73. Diachkova O O et al. *Opt. Commun.* **565** 130666 (2024)
74. Arkhipov R M *Bull. Lebedev Phys. Inst.* **51** (Suppl. 5) S365 (2024); *Kvantovaya Elektron.* **54** (2) 77 (2024)
75. Arkhipov R et al. *J. Opt. Soc. Am. B* **41** 1721 (2024)
76. Arkhipov R M, Arkhipov M V, Rosanov N N *JETP Lett.* **111** 484 (2020); *Pis'ma Zh. Eksp. Teor. Fiz.* **111** 586 (2020)